ELSEVIER

Brain Research 830 (1999) 218–225

BRAIN RESEARCH

Research report

Characterization of the neuroprotective and toxic effects of α7 nicotinic receptor activation in PC12 cells

Yangxin Li [a,1], Roger L. Papke [a,1], Yun-Ju He [b], William J. Millard [b], Edwin M. Meyer [a,*]

[a] *Department of Pharmacology and Therapeutics, University of Florida College of Medicine, Gainesville, FL, USA*
[b] *Department of Pharmacodynamics, University of Florida College of Pharmacy, Gainesville, FL, USA*

Accepted 9 March 1999

Abstract

The α7 nicotinic receptor partial agonist DMXB protected differentiated PC12 cells from NGF + serum deprivation over a concentration range (1–10 μM) that correlated with activation of protein kinase C. Increased toxicity was observed at a higher concentration of DMXB (30 μM) that did not elevate protein kinase C activity, but did increase tyrosine protein kinase activity. Neuroprotection was blocked with the protein kinase C-inhibitor bis-indolemaleimide, while toxicity was attenuated with the tyrosine protein kinase-antagonists herbimycin and genistein. The α7-selective antagonist methyllyconitine attenuated both the protective and toxic actions of DMXB, but in temporally distinct manners. Methyllyconitine (1 μM) attenuated toxicity when added 10 s before, but not 10 s after, 30 μM DMXB. In contrast, it blocked neuroprotection when added 10 min post-agonist addition. This temporal difference in receptor-activation that was necessary for protection vs. toxicity reflected the time courses for agonist-induced desensitization of the receptor expressed in *Xenopus* oocytes. These results indicate that α7 nicotinic receptors act through different intracellular transduction processes to protect or kill cells. Further, they suggest that the transduction processes may be differentially activated depending on the amplitude and duration of calcium signals.

Keywords: DMXB; Protein kinase C; Calcium; Tyrosine protein kinase; α7 Nicotinic receptor

1. Introduction

The α7 nicotinic receptor functions as an homo-oligomeric channel that is as permeant to calcium ions as excitotoxic NMDA receptors, but is much more rapidly desensitizing [5,25]. This receptor is found in a variety of brain regions, and is particularly concentrated in hippocampus and other telencephalic regions. It has been targeted therapeutically for Alzheimer's disease, based on studies with specific agonists such as 2,4-dimethoxybenzylideine anabaseine (DMXB, also known as GTS-21) that protect brain neurons as well as improve memory-related behaviors [18,19,27]. α7 receptors are activated by the transmitter acetylcholine (ACh) as well as the membrane phospholipid-breakdown product choline; this choline-activation is not observed with other nicotinic receptor subtypes [21]. The model systems in which selective activation of α7 nicotinic receptors prevents neuronal death are many, including focal ischemia [26], excitotoxic insults [1,27], trophic factor-deprivation [16,18,19], amyloid-exposure [12], and axotomy [16]. While information remains sparse about the intracellular processes underlying α7 nicotinic receptor-mediated neuroprotection, they are likely to be triggered by the receptor-mediated calcium-influx.

Two calcium-sensitive transduction systems that are associated with changes in cell viability are protein kinase C (PKC) and tyrosine protein kinase (TPK) [31]. PKC-activation has been associated with the anti-apoptotic effects of non-selective nicotinic receptor activation [32], so we investigated whether it may be involved in the DMXB-induced neuroprotection as well. Changes in TPK activity can also affect cell viability, though its role in nicotinic receptor-mediated neuroprotection has not been described [13,33]. This study used rat pheochromocytoma (PC12) cells that express α7 receptors [3] and are sensitive to the protective effects of DMXB during trophic factor deprivation [9,16,18,19].

* Corresponding author. Department of Pharmacology, J.H. Miller Health Center, Box 100267, Gainesville, FL 32610, USA. Fax: +1-352-392-9696

[1] These two authors contributed equally to this work.

0006-8993/99/$ - see front matter
PII: S0006-8993(99)01372-4

The possibility that over-activation of α7 nicotinic receptors may be neurotoxic was also considered. A previous study involving the expression of a mutated, non-desensitizing form of this receptor found reduced cell viability, apparently due to calcium-overloading [29]. Unpublished observations from our laboratory suggested that even cells expressing normal α7 receptors could be killed by acute application of high concentrations of nicotinic agonists. We therefore investigated the possible cytotoxic effect of high-dose DMXB in PC12 cells, as well as the roles of PKC and TPK activities in this toxicity.

The duration of receptor-activation necessary for cell loss was then compared to that required for neuroprotection using a selective receptor antagonist, methyllyconitine (MLA) [2]. Finally, the dose–response and temporal characteristics of α7 nicotinic receptor activation relative to cell viability and second messenger systems were compared to those seen in the *Xenopus laevis* oocyte expression system. This system effectively predicts the properties of α7 nicotinic receptors found in both peripheral and CNS neurons, e.g., with respect to rapid desensitization, high calcium permeability, pharmacological properties, and inward rectification [2,36]. Our results indicate that these receptor-properties are also consistent with the differential cellular actions of low- vs. high-dose DMXB in PC12 cells.

2. Materials and methods

2.1. Assessment of PC12 cell number and viability

PC12 cells were obtained from the original clonal line maintained at American Type Culture Collection (Rockville, MD). They were cultured and maintained as described previously [16,18]. Cultures were split at a 1:4 ratio every 3 days, up to eight passages, until differentiated was initiated with 100 ng/ml NGF. PC12 cell density was measured at 24 h or 4 days post-treatment for toxicity and protection studies, respectively, using the NIH Image 1.55 program. Five random photographs were analyzed in a blinded manner and values were normalized for differences in control densities. Values were expressed as means ± S.E.M. of at least 6 plates/group, over three separate experiments.

2.2. PKC assay

PKC activity was measured in membrane and soluble fractions of cell lysates obtained by sonication as described previously [17], using a kit purchased from Amersham (Arlington Heights, IL). This assay was based on the PKC-catalyzed transfer of the radio-labeled phosphate group of gamma-[^{32}P]ATP to a peptide that is specific for PKC. Cells were homogenized in a Tris buffer (50 mM Tris–HCl, pH 7.5 containing 5 mM EDTA, 10 mM EGTA with 0.3% w/v β-mercaptoethanol) containing 5 μg/ml leupeptin and 25 mg/ml aprotinin. Homogenates were centrifuged at $20\,000 \times g$ for 30 min at 4°C to separate membrane from cytosolic fractions. Each fraction was incubated for 15 min at 37°C on chromatography-grade paper in the assay buffer containing PKC-specific peptide, phosphatidylserine, dithiothreitol, and labelled ATP. Reactions were stopped by addition of orthophosphoric acid, and after washing the paper to remove unreacted [^{32}P]ATP, the ^{32}P-labelled peptide was quantified by liquid scintillation spectrophotometry.

2.3. TPK assay

TPK activity was measured using a non-radioactive ELISA based method purchased from Pierce (Rockford, IL). The biotinylated tyrosine kinase peptide was first bound to NeutrAvidin-coated wells, then tyrosine kinase-containing biological samples were added to the phosphorylate tyrosine residues. The anti™phosphotyrosine antibody, PY20, conjugated with horseradish peroxidase was added for specific detection of phosphotyrosine residues. TPK activity is detected by a soluble, one component, colorimetric substrate, 1-Step Turbo-TMB, that reacted with the HRP. Kinase activity was quantitated by comparison to a phosphopeptide curve.

2.4. Xenopus oocyte expression and recording

Preparation of in vitro synthesized cRNA transcripts and oocyte injection were described previously [6]. Recordings were made 4 to 7 days following mRNA injections. Current responses to drug administration were studied under two electrode voltage clamp at a holding potential of −50 mV. Recordings were made using a Warner Instruments oocyte amplifier interfaced with National Instruments' LabView software. Current electrodes were filled with 250 mM CsCl, 250 mM CsF and 100 mM EGTA, pH 7.3 and had resistances of 0.5–2.0 MΩ. Voltage electrodes were filled with 3 M KCl and had resistances of 1–3 MΩ. Oocytes with resting membrane potentials more depolarized than −30 mV were not used. Oocytes were perfused at room temperature with frog Ringer's (115 mM NaCl, 2.5 mM KCl, 10 mM HEPES pH 7.3, 1.8 mM $BaCl_2$) plus 1 μM atropine to block potential muscarinic responses. Barium was added to suppress calcium dependent chloride current contributing to integrated charge measurements. Drugs were diluted in perfusion solution and applied at a rate of 6 ml/min typical for oocyte-expression experiments [20,22]. Responses were normalized for the level of channel expression in each cell by measuring the response to a control application of 300 μM ACh when applied 5 min prior to the presentation of a test concentration of ACh or experimental agonists. Measurements of net charge were made by integration of the current responses for 200 s after the initial deflection from

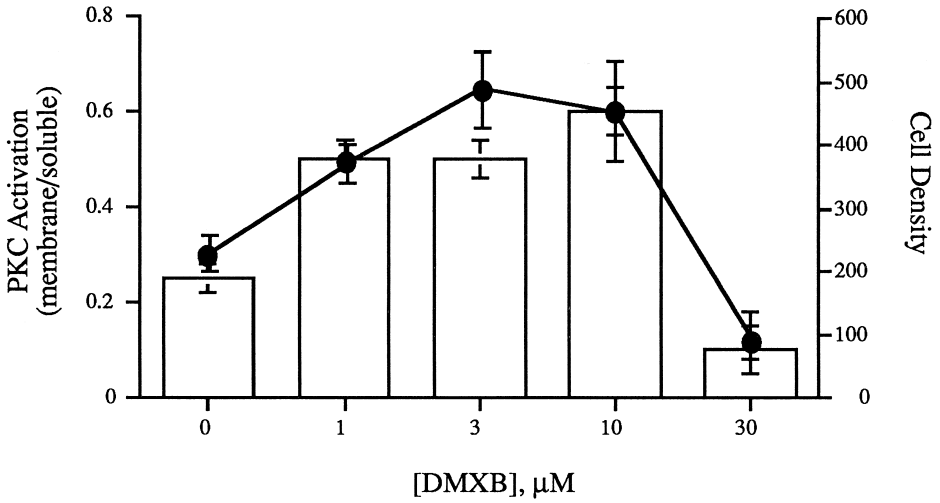

Fig. 1. Effects of α7 receptor activation on PKC activity and cell density in PC12 cells. Line refers to the ratio of membrane/cytosolic PKC activity 5 min after DMXB addition to PC12 cells. Bars refer to PC12 cell number/6 mm^2 measured 4 days after simultaneous addition of the drug and removal of NGF + serum. Results are mean ± S.E.M. of 4 plates/group; every PKC and cell density value was different from the drug-free control ($p < 0.05$; non-parametric *q*-test) [7].

baseline. Specifically, raw data values for experimental responses were imported into a template Excel spread sheet along with the raw data for the corresponding ACh controls obtained 5 min prior to the experimental response. Each record included a short (0.5 s) interval of baseline that was used for offset correction. Peaks and areas were then calculated for both the experimental and control responses, and the experimental values were expressed relative to the currents evoked by the control 300 μM ACh applications. Means and S.E.M. were calculated from the normalized responses of at least four oocytes for each experimental condition.

2.5. Measurement of intracellular calcium concentrations

Fluo-3/AM (Bio-Rad, Hercules, CA) was dissolved in dimethylsulfoxide (DMSO). Prior to addition of dye, PC12 cells were washed twice with PBS, gently removed from plates, and resuspended in a Hepes-buffered saline containing 140 mM NaCl, 5 mM KCl, 1 mM Na_2HPO_4, 5 mM glucose, 1 mM $CaCl_2$, 0.5 mM $MgCl_2$, 0.1% BSA, and 10 mM HEPES [30]. Fluo-3/AM was added to the suspension at a concentration of 3 μM and incubated for 30 min at room temperature. Cells were analyzed 2 min later fluorometrically with a FACScan flow cytometer (Beckton Dickinson, San Jose, CA). The threshold on the forward light scatter signal was adjusted to remove debris prior to collection. Excitation was from an argon laser at 488 nm. Emission at 530 ± 15 nm was measured on a log scale. Data were presented as the mean ± S.E.M. of relative fluorescent units of sample peak height. Since baseline values varied across different plates, each plate served as its own control, providing a baseline value immediately prior to addition of the drug. Statistical analyses used a paired *t*-test for samples vs. their respective baseline values; no multiple comparisons using the same data were performed.

3. Results

Removal of NGF and serum from differentiated PC12 cells reduced cell density in a manner that was attenuated by 1–10 μM DMXB but exacerbated by 30 μM DMXB (Fig. 1). DMXB also increased PKC-translocation to membrane binding sites in a concentration-dependent manner after a 5 min exposure (Fig. 1). That PKC-activation was important for the neuroprotective activity of DMXB was demonstrated with the cell-permeant PKC antagonist bisindole maleimide (BIM; [14]) (Table 1). This concentration of BIM was found to block PKC activity completely in PC12 cells treated in this manner (data not shown).

DMXB had no effect on TPK-activity at any concentration tested (1–30 μM) immediately after a 5 min treat-

Table 1
The effects of receptor and enzyme antagonists on DMXB-induced neuroprotection

Antagonist	Cell viability (% control)	
	Agonist	
	None	3 μM DMXB
None	100 ± 12	195 ± 35*
BIM	84 ± 7	78 ± 17[t]
Mecamylamine	109 ± 13	139 ± 9[t]

Differentiated PC12 cells were exposed to DMXB with or without 1 μM mecamylamine or 140 nM BIM, in the absence of NGF + serum. Untreated control value is density of surviving cells (220 cells/mm^2), mean ± S.E.M. of 4 plates/group.
* $p < 0.05$ compared to same treatment without agonist.
[t] $p < 0.05$ compared to same treatment without antagonist (non-parametric *q*-test) [7].

Table 2
The effects of enzyme antagonists on DMXB-induced neurotoxicity

Antagonist	Cell viability (% control)	
	Agonist	
	None	30 μM DMXB
None	100 ± 10	18 ± 2*
HERB	107 ± 14	57 ± 7*[t]
GEN	103 ± 12	53 ± 5*[t]

Non-differentiated PC12 cells were exposed to 0 or 30 μM DMXB with or without 5 μM HERB or 5 μM GEN. Cell density is expressed as the mean ± S.E.M. of 3–4 plates/group normalized to untreated plates assayed at the same time as the treatment. Untreated control cell density is 280 cells/6 mm^2.
* $p < 0.05$ compared to same treatment without agonist.
[t] $p < 0.05$ compared to same treatment without antagonist (non-parametric q-test) [7].

ment-interval (data not shown). However, after a 30 min exposure to the drug, there was an increase in TPK activity observed with 30 μM DMXB but not any lower, neuroprotective concentration (control vs. 30 μM DMXB-treated groups = 9.8 ± 0.9 vs. 18.9 ± 0.8 pmol of substrate phosphorylated/mg min; mean ± S.E.M.; $p < 0.05$ according to Student's t-test, $N = 6$ plates/group). Interestingly, this 30 μM DMXB-induced increase in TPK activity was completely blocked by 150 nM BIM (9.6 ± 0.07 pmol phosphorylated/mg min; mean ± S.E.M.), suggesting cross-talk between the PKC and TPK pathways in these cells. The TPK-antagonists herbimycin A (HERB) and genistein (GEN) [8,15] attenuated the cytotoxic actions of DMXB, suggesting a role for this kinase activity in the α7 receptor-mediated triggering of cell death (Table 2).

To investigate the duration of receptor activation necessary for cytoprotection and toxicity, 1 μM MLA was added at selected intervals before or after 3 μM or 30 μM DMXB. DMXB (30 μM)-induced reductions in PC12 cell viability were blocked when MLA was applied 10 s prior to, not 10 s after, the agonist (Fig. 2). Co-application of the

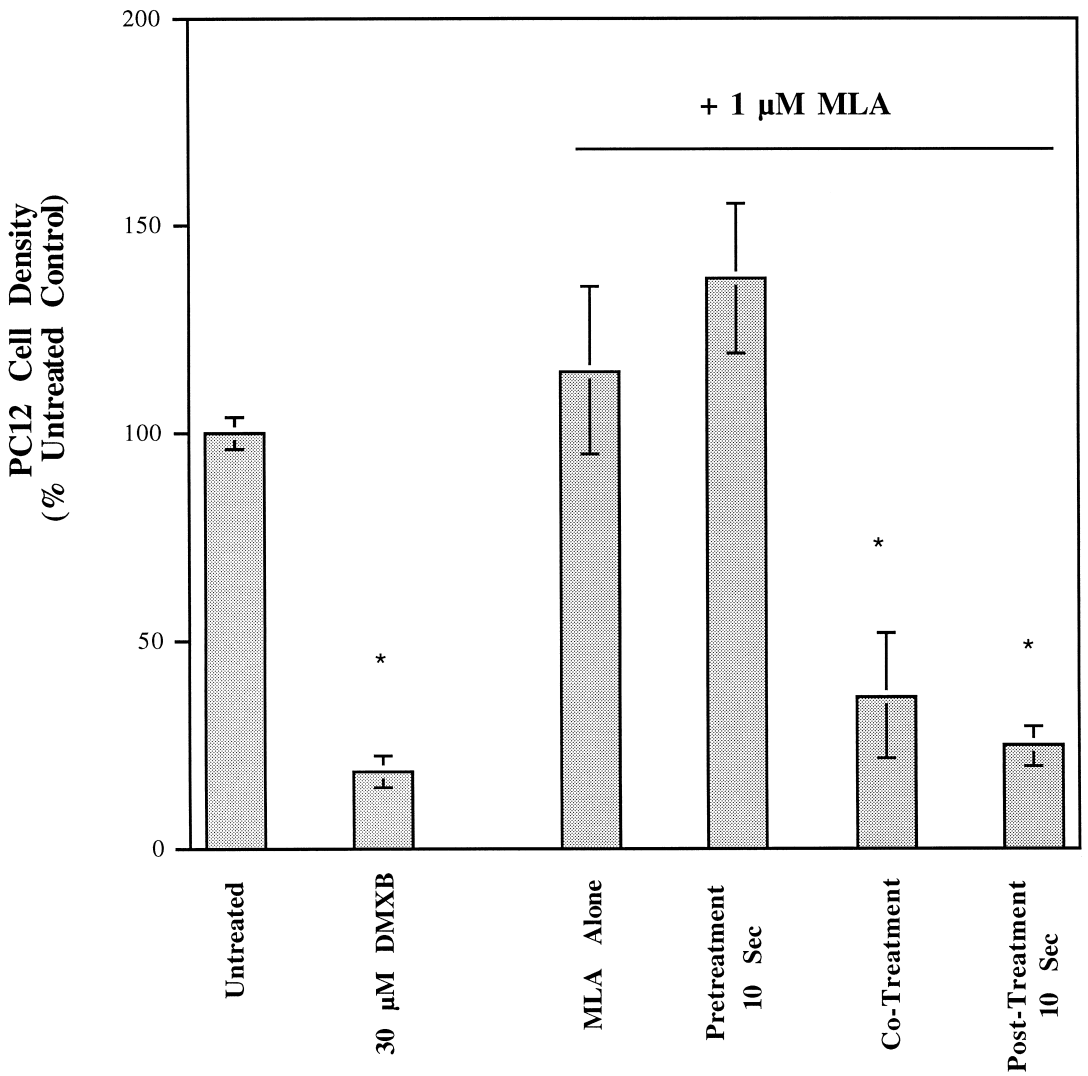

Fig. 2. MLA can antagonize the neurotoxic effects of a high concentration of DMXB on PC12 cell viability. PC12 cells were exposed to 0 (the 2 bars at the left) or 30 μM DMXB (the 4 bars at the right) together with, 10 s before, 10 s after MLA (1 μM). After 24 h, cell density was measured and expressed as the mean ± S.E.M. of 4 experiments/group, each in triplicate; * $p < 0.05$ vs. untreated group (non-parametric q-test) [7].

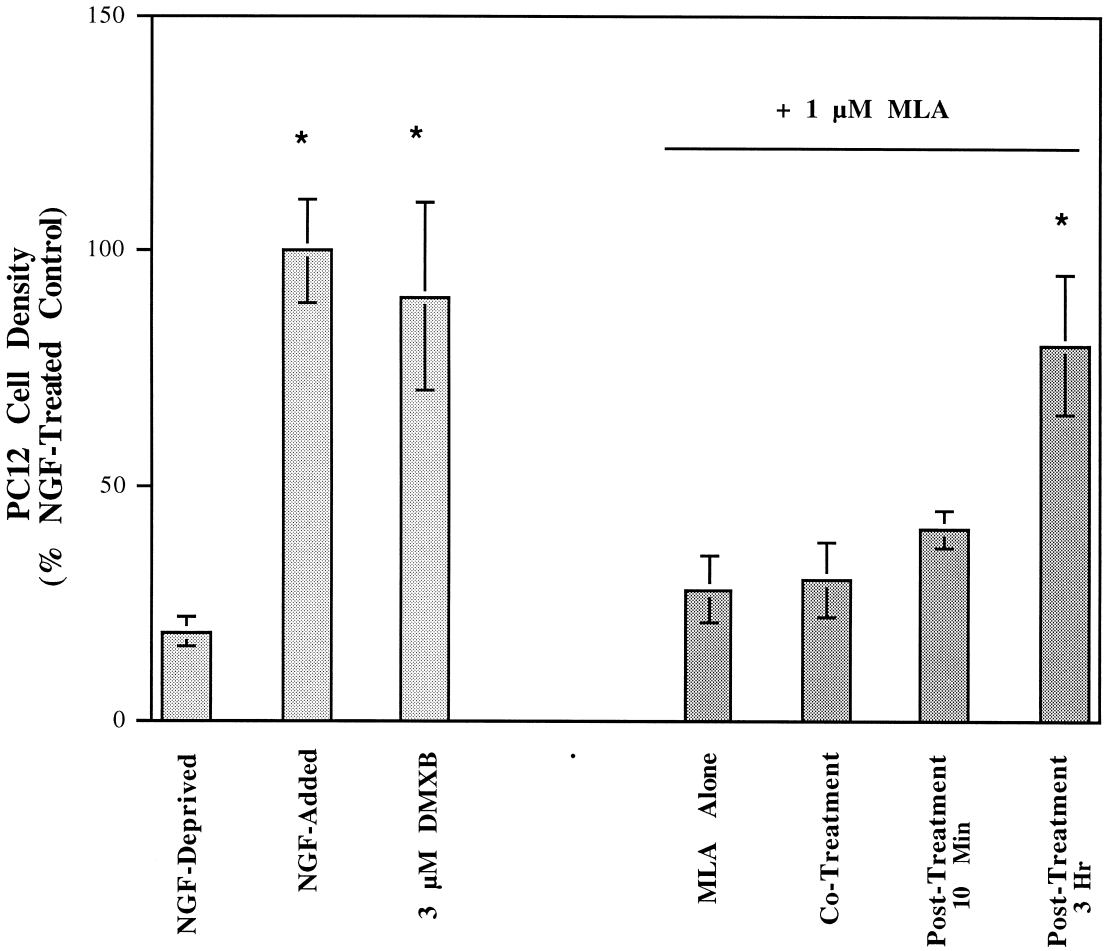

Fig. 3. MLA can antagonize the neuroprotective action of a low concentration of DMXB on PC12 cell viability. Differentiated PC12 cells were exposed to 0 or 3 μM DMXB immediately after the removal of NGF + serum, and cell density assayed as described in the text. MLA (1 μM) was added at the specified times relative to DMXB. Each value is the mean ± S.E.M. of four experiments, each conducted in duplicate, normalized to the 100 ng/ml NGF treated plates for the same experiment. $^{*}p < 0.05$ compared to NGF-treated group (positive control) (non-parametric q-test) [7].

agonist and antagonist gave intermediate, more variable, results. In contrast, the protection of PC12 cells with 3 μM DMXB required at least a 10-min, but not 3-h, activation of α7 receptors since MLA added at the former interval post-DMXB completely blocked this effect (Fig. 3).

The short (i.e., less than 10 s) exposure to 30 μM DMXB prior to receptor-blockade that was necessary to reduce PC12 cell density was consistent with receptor-kinetics observed in the *Xenopus* oocyte system. When DMXB was applied for 30 s at this high concentration, channel activity essentially ceased within a few seconds, indicating almost complete receptor desensitization (Fig. 4). It was unlikely that MLA would have any action once the receptors were predominantly in this desensitized state. In contrast, 3 μM DMXB increased α7 receptor-mediated currents for the entire duration of the recordings, at least 5 min. The protracted nature of the 3 μM DMXB-induced channel activation suggested a state in which a significant fraction of receptors could be activated by the agonist for an extended interval, i.e., had not been desensitized. Due to this difference in agonist-induced receptor-kinetics, the net ion influx induced by a 30 s DMXB application and measured over a 5 min interval differed only two-fold over this 10-fold concentration range (0.18 ± 0.01 and 0.37 ± 0.02 for 3 μM and 30 μM, respectively; $N = 4$ samples/group).

DMXB increased intracellular calcium-sensitive fluorescence in PC12 cells over a 2-min interval (Fig. 5). The DMXB-induced increase in Fluo3 was about three-folds greater in the 30 μM-exposed cells (186% of baseline values) than those exposed to 3 μM of the drug (126%). Over a 5-min interval, the effect of 3 μM DMXB on intracellular calcium concentrations was similar but did not reach statistical significance (118 ± 10% of baseline value; $p > 0.05$).

4. Discussion

The present study demonstrates that the degree of α7 nicotinic receptor activation can modulate cell viability in a dual manner that differentially involves PKC and TPK

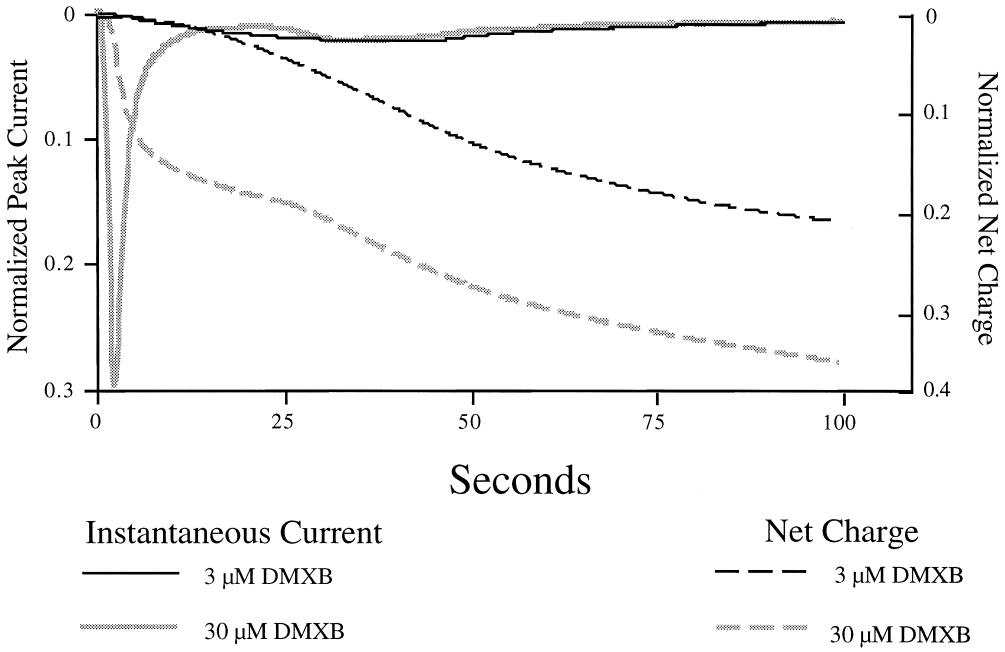

Fig. 4. Representative currents of rat α7 nAChR expressed in *Xenopus* oocytes for 30 s to 3 μM or 30 μM DMXB application. Data were normalized to the peak values from 300 μM ACh responses obtained in the same cell prior to DMXB.

activities. Neuroprotection is observed with low concentrations of DMXB that increase PKC translocation but that have no effect on TPK at any time point assayed up to 30 min. At least 10 min of low-level channel activation is necessary for neuroprotection conferred by 3 μM DMXB, which is consistent with the ongoing tonic activation of these receptors expressed in oocytes at this drug concentration. A neurotoxic concentration of DMXB, in contrast, triggers a brief, high amplitude pulse in receptor-activity in oocytes. It is also associated with a very different sequence of events intracellularly from that seen with 3 μM DMXB: no change in total PKC activation measured 5 min later, and a delayed increase in TPK activity that appears to require at least some PKC-activity (based on its BIM-sensitivity). The time-course for the antagonist effects of MLA on DMXB-induced neurotoxicity is consistent with a rapid onset of toxicity, with application of MLA 10 s post-agonist not effective. Interestingly, the co-application of MLA and DMXB had a significant, though somewhat variable, protective action. While this observation is difficult to interpret directly, because the relative on-rates for receptor binding of each agent (DMXB and MLA) are not known, it does indicate that this common experimental protocol would be likely to attenuate at some of the fast neurochemical actions of the agonist.

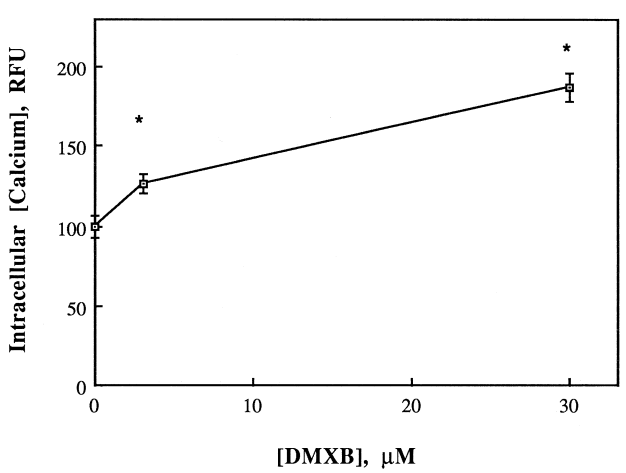

Fig. 5. Intracellular calcium-sensitive Fluo3 fluorescence in PC12 cells exposed to 3 or 30 μM DMXB for 2 min. Cells were loaded with 3 μM Fluo3/AM for 30 min, washed, and was added to the suspension at a concentration of 3 μM and incubated for 30 min at room temperature. Cells were analyzed for fluorescence at 488 nm/530 nm (excitation/emission) in a FACScan flow cytometer to obtain baseline values, then again 2 min after addition of the specified DMXB concentration. Results are mean ± S.E.M. of relative fluorescent units of sample peak height ($N = 3$ plates/group, each in duplicate). * $p < 0.05$ compared to respective baseline value, paired *t*-test.

Our results suggest that the DMXB-induced activation of PKC may be necessary for its neuroprotective action in this model of apoptosis based on its sensitivity to the selective antagonist BIM. Previously, activation of this enzyme system was reported to be sufficient to protect PC12 cells using low concentrations of phorbol esters [16,24]. The possibility that PKC activation underlies neuroprotection in this model is also consistent with other reports describing the role of this enzyme in cell viability. For example, nicotine-induced elevations in PKC activity are associated with the suppression of apoptosis in several endothelial cell lines [32]. Phorbol esters promote cell viability in PC12 cells [30], while PKC antagonists interfere with cell viability in a variety of systems, including

glioma cells [11] and primary cultures of rat cerebellar granule neurons [4].

The delayed TPK activation caused by a high concentration of DMXB may have been important for toxicity, which was blocked by the TPK-antagonists HERB or GEN. Unfortunately, no specific inhibitor exists for TPK activity, so it is possible that both HERB and GEN are acting through other mechanisms to interfere with this toxicity. Nonetheless, this observation agrees with reports that TPK inhibitors can inhibit apoptosis. GEN strongly attenuates NO-induced apoptosis in glomerular endothelial and mesangial cells [23]. HERB in turn abolishes cell death induced by Fas in T lymphocytes [28], and also inhibits DNA-fragmentation in K562 cells or HL-60 cells [34,35]. (However, see also [10].)

It is not clear why PKC activity was not elevated by 30 μM DMXB though the PKC-inhibitor BIM blocked the DMXB-induced activation of TPK. Two possible explanations are: (1) that high concentrations of DMXB differentially affect several PKC isozymes, yielding an overall unchanged amount of activity that hides an increase one or more of these isozymes; and (2) an activation of PKC occurred with the high DMXB concentration prior to sample collection for the assay, and this was followed by a partial down-regulation of activity by the 5 min interval. PKC down-regulation is a well established observation for several isozymes at high levels of activation (e.g., Ref. [17]).

It is interesting to compare the relative effects of DMXB on intracellular calcium accumulation measured in PC12 cells fluorometrically vs. those seen in the oocyte expression system. In each preparation, 3 μM DMXB caused a slight but detectable increase in signal over several min that was 0.35–0.5 that observed with a 10-fold higher concentration of DMXB. In the oocyte expression system, this lack of linearity can be shown to be due to the more rapid desensitization of the receptor at the higher DMXB concentration. It is likely that this is occurring in the PC12 cells as well, but a more detailed time-course for measuring changes in receptor-function would be necessary to demonstrate this.

In summary, specific α7 receptor activation can either protect or kill cells, depending on the level of activation. Protection is PKC-dependent, based on antagonist results, while toxicity is associated with TPK-activation. It is important to note that there has been no report of DMXB-induced neurotoxicity in vivo following its systemic administration, which may reflect the importance of its mode of application. DMXB may accumulate slowly enough in brain and other tissues following systemic administration in vivo to permit a large enough fraction of α7 nicotinic receptors to desensitize without the brief current-spike associated with neurotoxicity. In any case, the present results underline the need to evaluate both the toxic and protective actions of α7 agonists when considering their therapeutic efficacy, as well as the differential roles that low vs. high rates of receptor-activation play in these actions.

Acknowledgements

The authors appreciate the expert administrative assistance of Allison Dasta. This research was supported in part by NIA PO1 10485 and Taiho Pharmaceuticals, Japan.

References

[1] A. Akaike, Y. Tamura, Y. Takeharu, S. Shimohama, J. Kimura, Nicotine-induced protection of cultured cortical neurons against *N*-methyl-D-aspartate receptor-mediated glutamate cytotoxicity, Brain Res. 644 (1994) 181–187.

[2] M. Alkondon, E.F.R. Pereira, S. Wonnacott, E.X. Albuquerque, Blockade of nicotinic currents in hippocampal neurons defines methyllycaconitine as a potent and specific receptor antagonist, Mol. Pharmacol. 41 (1992) 802–808.

[3] E.M. Blumenthal, W.G. Conroy, S.J. Romano, P.D. Kassner, D.K. Berg, Detection of functional nicotinic receptors blocked by α-bungarotoxin on PC12 cells and dependence of their expression on post-translational events, J. Neurosci. 17 (1997) 6094–6104.

[4] C.M. Cagnoli, E. Kharlamov, C. Atabay, T. Uz, H. Manev, Apoptosis induced in neuronal cultures by the phosphatase inhibitor staurosporine is blocked by the isoquinolinesulfonamides H-7, H-8, and H-9, J. Mol. Neurosci. 7 (1996) 65–76.

[5] S. Couturier, D. Bertrand, J.M. Matter, M.C. Hernandez, S. Bertrand, N. Miller, V. Soledad, T. Barkas, M. Ballivet, A neuronal nicotinic acetylcholine receptor subunit (α7) is developmentally regulated and forms a homo-oligomeric channel blocked by α-bungarotoxin, Neuron 5 (1990) 8476–8486.

[6] C.M. de Fiebre, E.M. Meyer, W. Kem, R.L. Papke, Characterization of a family of anabaseine-derived compounds reveals that the 3-(4)-dimethylamino-cinnamylideine derivative is a selective agonist at neuronal nicotinic α7/α-bungarotoxin receptor subtypes, Mol. Pharmacol. 47 (1995) 164–171.

[7] W.J. Dixon, F.J. Massey, Jr., Introduction to Statistical Analysis, McGraw-Hill, New York, NY, 1969.

[8] H. Fukazawa, P.-M. Li, C. Yamamoto, Y. Murakami, S. Mizuno, Y. Uehara, Specific inhibitors of cytoplasmic protein tyrosine kinases by herbimycin A in vitro, Biochem. Pharmacol. 42 (1991) 1661–1671.

[9] L.A. Greene, A. Tischler, Establishment of a noradrenergic clonal line of rat adrenal pheochromocytoma cells which respond to nerve growth factor, Proc. Natl. Acad. Sci. USA 73 (1976) 2424–2428.

[10] L. Hunakova, M. Sulikova, J. Duraj, J. Sedlak, B. Chorvath, Stimulation of 1-(beta-D-arabinofuranosyl) cytosine (AraC)-induced apoptosis in the multidrug resistant human promyelocytic leukemia cell lines with protein kinase inhibitors, Neoplasma 43 (1996) 291–295.

[11] S. Kawecki, The effect of calphostin C, a potent photodependent protein kinase C inhibitor, on the proliferation of glioma cells in vitro, J. Neurooncol. 31 (1997) 255–266.

[12] T. Kihara, S. Shimohama, H. Sawada, J. Kimura, T. Kume, H. Kochiyama, T. Maeda, A. Akaike, Nicotinic receptor stimulation protects neurons against beta-amyloid toxicity, Ann. Neurol. 42 (1997) 159–163.

[13] M.S. Kindy, Inhibition of tyrosine phosphorylation prevents delayed neuronal death following cerebral ischemia, J. Cereb. Blood Flow Metab. 13 (1993) 372–377.

[14] J. Kirilovsky, The bisindolylmaleimide GF 109203X is a potent and selective inhibitor of protein kinase C, J. Biol. Chem. 266 (1993) 15771–15781.

[15] B.M. Koroma, E. de-Juan Jr., Phosphotyrosine inhibition and control of vascular endothelial cell proliferation by genistein, Biochem. Pharmacol. 48 (1994) 809–818.
[16] E.J. Martin, K.S. Panicker, M.A. King, M. Deyrup, B.E. Hunter, E.M. Meyer, Cytoprotective action of 2,4-dimethoxybenzylidene anabaseine in differentiated PC12 cells and septal cholinergic neurons, Drug Dev. Res. 31 (1994) 127–134.
[17] E.M. Meyer, E.O. Hardwick, J.H. Judkins, Effects of peroxidation and aging on acetylcholine release and protein kinase C activity, Neurobiol. Aging 15 (1994) 63–67.
[18] E.M. Meyer, E.T. Tay, R.L. Papke, C. Meyers, G.L. Huang, C.M. de Fiebre, [2,4-dimethoxybenzylidene]anabaseine (DMXB) selectively activates rat α7 receptors and improves memory-related behaviors in a mecamylamine-sensitive manner, Brain Res. 768 (1997) 49–56.
[19] E.M. Meyer, E.T. Tay, J.A. Zoltewicz, C. Meyers, M.A. King, R.L. Papke, C.M. de Fiebre, Neuroprotective and memory-related actions of novel α7 nicotinic agents with different mixed agonist/antagonist properties, J. Pharmacol. Exp. Ther. 284 (1998) 1026–1032.
[20] R.L. Papke, S.F. Heinemann, The partial agonist properties of cytisine on neuronal nicotinic receptors containing the β_2 subunit, Mol. Pharm. 268 (1999) 718–726.
[21] R.L. Papke, M. Bencherif, P. Lippiello, An evaluation of neuronal nicotinic acetylcholine receptor activation by quaternary nitrogen compounds indicates that choline is selective for the α7 subtype, Neurosci. Lett. 213 (1996) 201–204.
[22] R.L. Papke, J.S. Thinschmidt, B.A. Moulton, E.M. Meyer, A. Poirier, Activation and inhibition of rat neuronal nicotinic receptors by ABT-418, Br. J. Pharmacol. 120 (1997) 429–438.
[23] J. Pfeilschifter, A. Huwiler, Nitric oxide stimulates stress-activated protein kinases in glomerular endothelial and mesangial cells, FEBS Lett. 396 (1996) 67–70.
[24] A. Rukenstein, R.E. Rydel, L.A. Greene, Multiple agents rescue PC12 cells from serum free cell death by translation and transcription independent mechanisms, J. Neurosci. 11 (1991) 2552–2563.
[25] P. Seguela, J. Wadiche, K. Dineley-Miller, J.A. Dani, J.W. Patrick, Molecular cloning, functional properties and distribution of rat brain α7: a nicotinic cation channel highly permeable to calcium, J. Neurosci. 13 (1993) 595–604.
[26] S. Simuzu, K. Umezawa, M. Takada, N. Arber, M. Imoto, Induction of hydrogen peroxide production and Bax expression by caspase-3-(-like) proteases in tyrosine kinase inhibitor-induced apoptosis in human small cell lung carcinoma cells, Exp. Cell Res. 238 (1998) 197–203.
[27] S. Shimohama, A. Day, D. Greenwald, D. Shafron, C. Simpkins, E.M. Meyer, α7 nicotinic receptor activation protects against NMDA-induced toxicity in vitro and focal ischemia induced neurotoxicity, Brain Res. 779 (1998) 359–363.
[28] I. Szabo, E. Gulbins, H. Apfel, X. Zhang, P. Barth, A.E. Busch, K. Schlottmann, O. Pongs, F. Lang, Tyrosine phosphorylation-dependent suppression of a voltage-gated K^+ channel in T lymphocytes upon Fas stimulation, J. Biol. Chem. 271 (1996) 20465–20469.
[29] M. Treinin, M. Chalfie, A mutated acetylcholine receptor subunit causes neuronal degeneration in *C. elegans*, Neuron 14 (1995) 871–877.
[30] P.A. Vandenberghe, J.L. Ceuppens, Flow cytometric measurement of cytoplasmic free calcium in human peripheral blood T lymphocytes with Fluo-3, a new fluorescent calcium indicator, J. Immunol. Meth. 127 (1990) 197–205.
[31] P.R. Walker, J. Kwast-Welfeld, H. Gourdeau, J. Leblanc, W. Neugebauer, M. Sikorska, Relationship between apoptosis and the cell cycle in lymphocytes: roles of protein kinase C, tyrosine phosphorylation, and AP1, Exp. Cell Res. 207 (1993) 142–151.
[32] S.C. Wright, J. Zhong, H. Zheng, J.W. Larrick, Nicotine inhibition of apoptosis suggests a role in tumor promotion, FASEB J. 7 (1993) 1045–1051.
[33] L.W. Wu, P.B. Hackett, Development of cellular resistance to pp60 v-src kinase-induced cell death, Oncogene 11 (1995) 1459–1468.
[34] M. Yabuki, Y. Inai, T. Yoshioka, K. Hamazaki, T. Yazuda, M. Inoue, K. Utsumi, Oxygen-dependent fragmentation of cellular DNA by nitric oxide, Free Radic. Res. 26 (1997) 245–255.
[35] A. Yamauchi, K. Taga, H.S. Mostowski, E.T. Bloom, Target cell-induced apoptosis of interleukin-2-activated human natural killer cells: roles of cell surface molecules and intracellular events, Blood 87 (1996) 5127–5135.
[36] Z. Zhang, J.S. Coggan, D.K. Berg, Synaptic currents generated by neuronal acetylcholine receptors sensitive to α-bungarotoxin, Neuron 17 (1996) 1231–1240.